Rate Coefficients for Reactions of NO_3 with a Few Olefins and Oxygenated Olefins

Yinon Rudich,[†] Ranajit K. Talukdar,[‡] R. W. Fox,[§] and A. R. Ravishankara*[,‡,||]

Aeronomy Laboratory, National Oceanic and Atmospheric Administration, Boulder, Colorado 80303

Received: October 17, 1995; In Final Form: January 11, 1996[⊗]

The rate coefficients for the reactions of NO_3 with 2-methyl-3-butene-2-ol (methyl butenol, MBO, k_1), 1-butene (k_2), *trans*-2-butene (k_3), methacrolein (MACR, k_4), and methyl vinyl ketone (MVK, k_5) were measured directly using a flow tube coupled to a diode laser absorption system where NO_3 was measured. The measured values of the rate coefficients are $k_1 = 4.6 \times 10^{-14} \exp(-400/T)$ cm^3 molecule^{-1} s^{-1}, $k_2 = 5.2 \times 10^{-13} \exp(-1070/T)$ cm^3 molecule^{-1} s^{-1}, $k_3(298\ \text{K}) = (4.06 \pm 0.36) \times 10^{-13}$ cm^3 molecule^{-1} s^{-1}, $k_4(298\ \text{K}) \leq 8 \times 10^{-15}$ cm^3 molecule^{-1} s^{-1}, and $k_5(298\ \text{K}) \leq 1.2 \times 10^{-16}$ cm^3 molecule^{-1} s^{-1}. The observed reactivity trends are correlated in terms of the presence of electron-withdrawing substituents, which reduces the reactivity of alkenes toward NO_3 addition to the double bond. The contribution of NO_3 reactions to determining the tropospheric lifetimes of these compounds are also calculated.

Introduction

The nighttime reactions of the nitrate radical, NO_3, with unsaturated hydrocarbons can be a major loss channel for these compounds in the troposphere.[1] For some hydrocarbons, the oxidation by NO_3 can be as significant as the daytime reaction with the OH radical. The relatively large rate coefficients of the NO_3 reactions and the high concentration of the nitrate radical make the removal by NO_3 competitive. Characterization of the NO_3 reactions with unsaturated hydrocarbons is needed for understanding the tropospheric chemistry of alkenes and that of the NO_3 radical.

The NO_3 reactions with alkanes, which proceed by hydrogen atom abstraction, are slow, with tertiary H atom abstraction being faster than secondary H atom abstraction, which is faster than the abstraction of a primary H atom.[2] The reactions of NO_3 with alkenes are usually $\gtrsim$2 orders of magnitude faster than those with alkanes. The rate coefficients for the reactions of alkenes with NO_3 span about 5 orders of magnitude from the reactions of the 1-alkenes ($k = 2 \times 10^{-16}$ cm^3 molecule^{-1} s^{-1} for ethene) to the more substituted alkenes ($k = 5.7 \times 10^{-11}$ cm^3 molecule^{-1} s^{-1} for 2,3-dimethyl-2-butene).[2] The increase in the rate coefficients is similar to that in OH reactions, which proceed at low temperatures predominantly by addition to the C=C double bond. Abstraction from side alkyl chains is probably not important at atmospheric temperatures, as can be deduced from the much smaller rate coefficients for alkanes.[3]

Under atmospheric conditions, the hydrocarbon degradation initiated by NO_3 attack can lead to formation of nitrato peroxynitrates and dinitrates. These thermally unstable compounds can be transported from polluted to rural and relatively clean areas and serve as reservoir species to the peroxy radicals and to reactive nitrogen.

In a recent field campaign,[4] 2-methyl-3-butene-2-ol ($CH_3COH(CH_3)CHCH_2$, methyl butenol, MBO) was identified as an important emission from vegetation, which can be present in the atmosphere at high concentrations. The origin of MBO in the troposphere is still uncertain, but its concentration can sometimes exceed that of isoprene,[4] which suggests that MBO may play an important role in tropospheric chemistry by influencing tropospheric ozone buildup[5,6] and transport of reactive species in the boundary layer.[7] To characterize MBO's atmospheric fate, we recently measured its absorption cross section in the wavelength region relevant to the troposphere and the rate coefficient for its reaction with the OH radical.[8] We found the photolysis rate of MBO to be negligibly small, while its reaction with OH to be fast. Grosjean and Grosjean[9] measured the rate coefficient for the reaction of ozone with MBO to be 1×10^{-17} cm^3 molecule^{-1} s^{-1} at 291 K. On the basis of these results, we concluded[8] that the main loss mechanism for MBO in the atmosphere during the day is its reaction with the OH free radical. This process leads to an atmospheric lifetime of less than 5 h.

To quantify the loss of MBO at nighttime we have measured the rate coefficient for the reaction of MBO with NO_3

$$\text{2-methyl-3-butene-2-ol} + NO_3 \xrightarrow{k_1} \text{products} \qquad (1)$$

between 258 and 396 K. In addition we have investigated the reactions of NO_3 with other olefins:

$$\text{1-butene} + NO_3 \xrightarrow{k_2} \text{products} \qquad (2)$$

$$\textit{trans}\text{-2-butene} + NO_3 \xrightarrow{k_3} \text{products} \qquad (3)$$

$$\text{MVK} + NO_3 \xrightarrow{k_4} \text{products} \qquad (4)$$

$$\text{MACR} + NO_3 \xrightarrow{k_5} \text{products} \qquad (5)$$

where MVK is methyl vinyl ketone and MACR is methacrolein. k_2 was measured over a wide range of temperatures (between 232 and 401 K), while k_3 was measured at a few temperatures. Reactions 2 and 3, which have been studied before, also served as a test of a new flow tube combined with a diode laser absorption system used to measure the rate coefficients of NO_3 reaction with MBO. Since k_4 and k_5 were very small, we could only report upper limits for these values.

The observed reactivity trends are discussed in terms of the substituent groups, especially oxygen-containing functional

[†] NOAA/National Research Council Postdoctoral Research Associate.
[‡] Also affiliated with the Cooperative Institute for Research in Environmental Sciences, University of Colorado, Boulder, Colorado 80309.
[§] National Institute of Standards and Technology, Time and Frequency Division, Boulder, Colorado 80303.
[||] Also associated with the Department of Chemistry and Biochemistry, University of Colorado, Boulder, Colorado 80303.
[⊗] Abstract published in *Advance ACS Abstracts,* March 1, 1996.

0022-3654/96/20100-5374$12.00/0

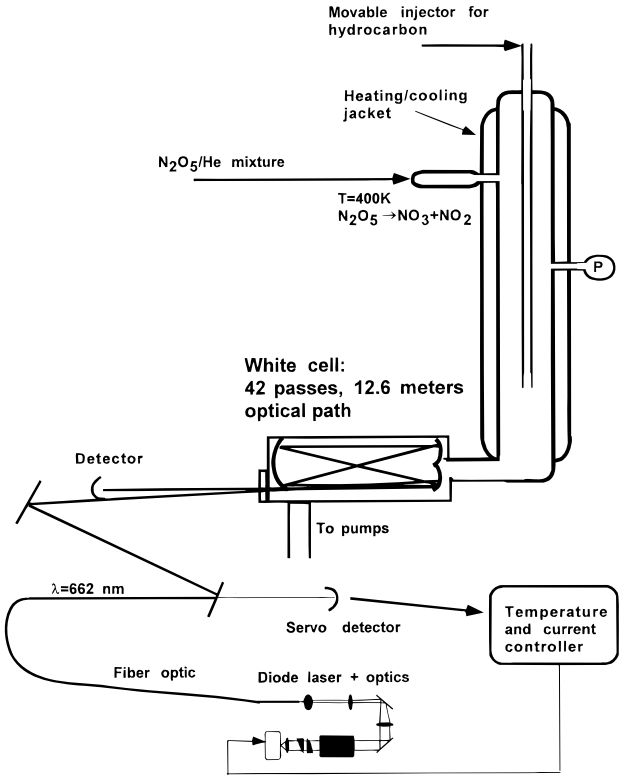

Figure 1. Schematic diagram of the experimental setup, showing the diode laser system, White cell, and the flow tube.

groups. We also discuss the importance of NO_3 reactions relative to other loss processes of unsaturated organic compounds in the atmosphere.

Experimental Section

A schematic diagram of the apparatus used to study reactions 1−5 is shown in Figure 1. A jacketed flow tube equipped with a movable injector was used. Heated or cooled liquid from a constant temperature bath was flowed through the jacket to control the temperature of the flow tube between 230 and 400 K. The temperature was measured using a retractable thermocouple. The flow tube had an internal diameter of 2.54 cm. The inner wall of the tube was used bare ($T > 298$ K), with a Teflon sleeve (at some of the high- and low-temperatures experiments), or with a halocarbon wax coating (at $T < 298$ K). The pressure in the reactor was measured using a 10 Torr (1330 Pa) capacitance manometer at the center of the reactor. Typical pressure during the experiments was 1.5−3 Torr (200−400 Pa); on occasions, pressures up to ∼15 Torr (2000 Pa) were used.

NO_3 absorption was detected using a visible tunable diode laser combined with a White cell[10,11] with a base path length of 30 cm and 42 passes to obtain a total absorption path length of 12.6 meter. The multipass cell was in a glass jacket with an inner diameter of 2.3 cm and a total volume of about 130 cm^3. The mirrors had a dielectric coating with a reflectance of >99% between 450 and 700 nm. To measure I_0, the intensity of light without NO_3, NO was added to the gas flow at the entrance to the cell to completely titrate away NO_3.

The temperature and current of the diode laser were adjusted to operate in a single mode near 661.9 nm, the peak of the NO_3 absorption.[1] An optical fiber was used to spatially filter and transmit the beam to the White cell. To minimize optical feedback-induced amplitude noise, the fiber ends were polished at an 8° angle and the beam was passed through an optical isolator. Approximately 60% of the laser power (∼4 mW total power) was coupled into the fiber by using a spherical lens, an anamorphic prism pair, and a telescope (×3) in addition to the collimating and focusing objectives.

At the fiber output, approximately 50% of the power was directed to a photodiode for an amplitude stabilization servo. A stable offset current was subtracted from the photocurrent to provide an error signal and then fed back to the laser's injection current with a bandwidth of 100 kHz. The offset current was derived from a stable, well-filtered voltage reference and a precision resistor with a low temperature coefficient. The remaining laser power was then mode-matched to the waist of the White cell, and the cell output was directed to the signal photodiode.

The fiber caused the beam polarization to vary slightly with temperature and acoustic noise, which resulted in amplitude noise on the signal photocurrent due to the polarization sensitivity of the optics. This was eliminated by using a polarizer immediately after the collimated fiber output before sampling the beam for the servo.

The laser's wavelength was initially tuned to the NO_3 absorption line using a diode array spectrometer calibrated using a Ne lamp. The correction current for the amplitude stabilization (<0.1 mA) did not significantly change the wavelength, and the laser's spectrum was periodically checked with the spectrometer or with an optical multichannel analyzer to ensure single-mode operation.

The output of the signal detector was read by a digital voltmeter, averaged with about a 3 s time constant, and monitored by a computer for further analysis. The stability of the detection system, as measured by the fluctuations in the intensity, was about 1×10^{-4}; it was limited by vibrations of the multipass cell. This stability corresponds to a sensitivity of $\sim 4 \times 10^9$ molecules cm^{-3}, using an absorption cross section of NO_3 at 662 nm[1] of $\sigma(662\text{ nm}) = 2 \times 10^{-17}$ cm^2.

NO_3, prepared by thermal decomposition of N_2O_5

$$N_2O_5 \xrightarrow{M} NO_3 + NO_2 \qquad (6)$$

in a 20 cm long, 10 cm i.d oven heated to ∼400 K, was flowed into the flow tube through a side arm. The pressure inside the oven was controlled using a Teflon stopcock and was usually in the range 3.5−6 Torr (470−800 Pa). Under these conditions, reaction 6 went to completion in a time much shorter than the residence time in the reactor. In a few experiments, the F + HNO_3 reaction was also used as an NO_3 source, but the thermal decomposition source was preferred because it is cleaner, i.e., it does not produce many other significant reactive species.

In all experiments at $T > 298$ K, the measured NO_3 loss on the movable injector was less than 1 s^{-1}. In a separate set of experiments, the rate constant for loss of NO_3 on the main flow tube wall was measured by adding NO_3 through the movable injector to be less than 2 s^{-1}. In the presence of the olefin reactant, first-order rate constants of up to 70 s^{-1} were observed. At $T < 298$ K, wall-catalyzed reactions contributed significantly to the loss of NO_3 as indicated by nonexponential temporal profiles and nonzero intercepts in the plots of measured first-order rate constant vs [reactant]. Halocarbon wax coating minimized the wall losses at lower temperatures.

In a typical experiment, NO_3 was flowed through the reactor and its concentration was measured. Then the alkene was introduced through the movable injector and the NO_3 concentration was measured for various reaction distances, which were varied by moving the injector.

High-purity gases (He (>99.9995%), O_2 (99.995%), 1-butene (>99%), *trans*-2-butene (>99%), and NO (99.9%)) were used as supplied. Commercially available MBO, MACR, and MVK were transferred to glass bulbs and were directly flowed to the reactor. Concentrations of all the gases were determined by using calibrated electronic mass flow meters.

N_2O_5 was synthesized by the reaction of ozone with NO_2. Ozone was prepared by a commercial ozone generator using high-purity (>99.995%) oxygen flowed through a molecular sieve trap at 195 K. The ozone/O_2 mixture from the ozone generator was mixed with NO_2, which was formed in situ by the reaction of O_2 with pure NO. High-purity NO was obtained by passing the gas through a silica gel trap immersed in a dry ice/ethanol bath (195 K), which removes higher nitrogen oxides. The gases were mixed in a 50 cm long, 3.8 cm inner diameter reactor at a pressure of 800 Torr (1.07×10^5 Pa), and the resulting gas mixture was passed through a trap held at dry ice/ethanol temperature to collect N_2O_5. During the experiments, the N_2O_5 was flushed out of the trap, which was maintained at ~215 K, by high-purity He.

Results

Reactions 1−5 were studied under pseudo-first-order conditions, with [alkene]/[NO_3] ~ 50−1000. Under these conditions, the NO_3 decay obeyed first-order kinetics, i.e.,

$$[NO_3]_z = [NO_3]_{z_0} e^{-k'[(z/\omega)-(z_0/\omega)]} \quad (1)$$

where $[NO_3]_z$ and $[NO_3]_{z_0}$ are the concentrations of NO_3 at distances z and z_0, ω is the flow velocity of the gases in the flow tube, and k' is the pseudo-first-order loss rate coefficient due to all reactive processes. The relative reaction times, $t - t_0 = (1/\omega)(z - z_0)$, were calculated from the injector position and the computed flow velocities ω. The flow velocities were corrected for the viscous pressure drop down the tube.[12,13] The first-order loss rate coefficients, k'_i, were measured as a function of concentration of the reactant. A linear least squares fit of k'_i vs [alkene] gave the second-order rate coefficients k_i. The k_i values were plotted as a function of $1/T$ to obtain the Arrhenius parameters A and E_a/R according to eq 2

$$k_i(T) = A e^{-(E_a/(RT))} \quad (2)$$

where E_a is the activation energy for the reaction, A is the Arrhenius pre-exponential factor, and R is the gas constant.

We believe that the main source of error in the experiments results from uncertainties in the determination of the concentration of the olefin in the flow tube. We estimate this error to be not more than 7% at the 95% confidence level. The estimated uncertainty, which includes both precision and estimated systematic errors, for the rate coefficient at temperature T is expressed using the commonly used formula in rate data evaluations, for example, the NASA/JPL evaluation[14]

$$f(T) = f(298) e^{|(\Delta E_a/R)((1/T)-(1/298))|} \quad (3)$$

In eq 3, which can be used for calculating the uncertainty in the value of k at temperature T, $f(298)$ is the estimated uncertainty in the value of the rate coefficient at 298 K and was derived using $k(298\ K)$ calculated from the Arrhenius parameters and the measured values near 298 K. (It is implicitly assumed that the rate coefficient at 298 K is the best defined value.) ΔE_a is chosen to estimate the uncertainty in the rate coefficients at T ≠ 298 K.

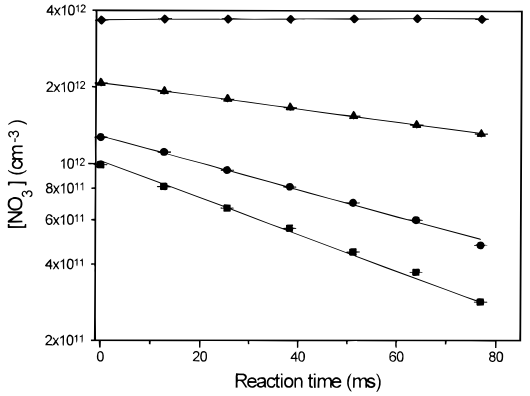

Figure 2. Example for the first-order decays of NO_3 for various MBO concentrations at $T = 296$ K: ◆, no MBO added; ▲, [MBO] = 5×10^{14} cm^{-3}; ●, [MBO] = 1×10^{15} cm^{-3}; ■, [MBO] = 1.4×10^{15} cm^{-3}. The decays are exponential, as is expected for pseudo-first-order conditions, in the absence of secondary reactions.

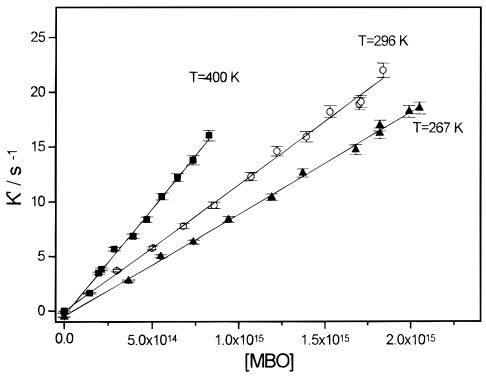

Figure 3. Plots of pseudo-first-order rate constants for reaction 1: ■, 400 K; ○, 296 K; ▲, 267 K. The slopes of these plots give the rate coefficient $k_1(T)$ at a given temperature T.

***trans*-2-Butene + NO_3.** As a check of the new experimental apparatus, we measured k_3 at 298 and 267 K. Reaction 3 was chosen for comparison because *trans*-2-butene has a structure close to that of the other molecules that we studied and its rate coefficient for the reaction with NO_3 is well established.[2,15] The results [$k_3(298\ K) = (4.06 \pm 0.36) \times 10^{-13}$ and $k_3(267\ K) = (3.55 \pm 0.33) \times 10^{-13}$ cm^3 molecule^{-1} s^{-1}] are in excellent agreement with the value recommended by Atkinson[2] [$k_3(298\ K) = 3.9 \times 10^{-13}$ cm^3 molecule^{-1} s^{-1}] and with those measured by Dlugokencky *et al.*[15] in a fast flow system with laser-induced fluorescence (LIF) detection of the NO_3 reactant[15] ($k_3(298\ K) = (3.96 \pm 0.06) \times 10^{-13}$, $k_3(267\ K) = (3.55 \pm 0.04) \times 10^{-13}$ cm^3 molecule^{-1} s^{-1}). To our knowledge, Dlugokencky *et al.* are the only ones who have previously measured the temperature dependence of this rate coefficient.

2-Methyl-3-butene-2-ol + NO_3. Typical NO_3 temporal profiles for reaction 1 are shown in Figure 2. In addition, plots of the pseudo-first-order rate coefficients (k'_1) vs [MBO] are shown in Figure 3 for three different temperatures. The measured rate coefficients, along with pertinent experimental conditions, are listed in Table 1. The values of k_1 measured between 258 and 397 K are also shown in Figure 4 (solid squares) in the Arrhenius form [eq 2]. The line in Figure 4 is a fit of the data to eq 2 between 267 and 396 K and corresponds to the Arrhenius parameters given in Table 3: $A = 4.6 \times 10^{-14}$ cm^3 molecule^{-1} s^{-1}, $E_a = -800$ cal mol^{-1}, $\Delta E_a = 70$ cal mol^{-1}, and $f(298) = 1.07$. The recommended rate coefficient at 298 K, $k_1(298\ K)$, is $(1.21 \pm 0.09) \times 10^{-14}$ cm^3 molecule^{-1} s^{-1}. All the quoted uncertainties are at the 95% confidence level.

TABLE 1: Rate Coefficients (in Units of cm^3 molecule^{-1} s^{-1}) for Reaction 1 and Pertinent Experimental Conditions[a]

temp (K)	10^{14} × rate coefficient	pressure (Torr)	flow velocity (cm s^{-1})	[MBO]/[NO_3]	wall coating
267	0.95 ± 0.08	2	350	130−714	wax[b]
280	1.09 ± 0.09	2	615	55−350	wax[b]
295	1.2 ± 0.09	1.2	376	100−620	wax[b]
296	1.14 ± 0.09	8.8	301	170−650	Teflon
296	1.14 ± 0.09	2.6	840	45−450	wax[b]
296	1.30 ± 0.09	2.6	622	72−390	none
297	1.23 ± 0.09	2.5	680	95−500	none
297	1.26 ± 0.09	2.5	750	65−360	none
297	1.23 ± 0.09	2.4	880	90−500	Teflon
313	1.29 ± 0.10	2.5	1034	40−224	Teflon
313	1.27 ± 0.10	2.7	660	74−410	none
314	1.27 ± 0.10	2.7	750	50−350	none
314	1.22 ± 0.10	2.5	712	72−400	none
333	1.44 ± 0.12	2.5	740	80−475	none
346	1.35 ± 0.12	2.5	1120	30−200	Teflon
351	1.58 ± 0.13	2.7	733	62−400	none
353	1.42 ± 0.13	2.7	740	61−360	none
365	1.44 ± 0.13	2.5	1165	34−215	Teflon
373	1.52 ± 0.14	2.5	780	50−350	none
373	1.52 ± 0.14	2.7	800	53−300	none
400	1.76 ± 0.18	2.5	650	60−320	none
400	1.76 ± 0.18	2.7	830	50−280	none

[a] The error bars include precision and estimated systematic (2σ) errors. [b] Wax = halocarbon wax.

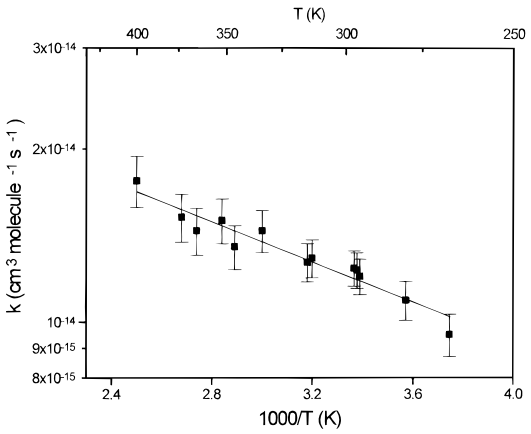

Figure 4. Plots of k_1 (log scale) vs $1/T$ for the reaction of MBO + NO_3. The line is a weighted fit of the data to the Arrhenius expression. The error bars include precision and estimated systematic errors, as mentioned in the text. The data obtained at low temperatures using uncoated or Teflon coated walls are not included.

At temperatures lower than 290 K, the measured values of k_1 on uncoated flow tube walls deviated from the behavior expected from eq 2. When a Teflon sleeve was inserted into the flow tube to minimize wall losses, eq 2 was obeyed down to 280 K. With halocarbon wax, eq 2 was obeyed down to 260 K. However, in the absence of MBO, the first-order loss rate coefficients of NO_3 on the injector were always less than 1 s^{-1} at all temperatures. We attribute the sharp deviation from eq 2 at low temperatures to enhanced reactive loss of NO_3 due to heterogeneous reaction of NO_3 with MBO sticking on the walls of the flow tube. This view is supported by the change in the temperature at which deviation from eq 2 is observed with the character of the wall surface. Since MBO has a somewhat low vapor pressure (∼25 Torr at 298 K) and a polar OH group, it is expected to be "sticky" on the flow tube walls where it can react heterogeneously with NO_3. Therefore, we did not include data obtained below 260 K in our fit to eq 2.

In addition to experiments at the usual ∼2 Torr (367 Pa) pressure, we measured k_1 at pressures of 10−15 Torr (1330−2000 Pa). No significant change in k_1 was observed. Furthermore, k_1 did not change upon addition of oxygen (up to 1 Torr (133 Pa)).

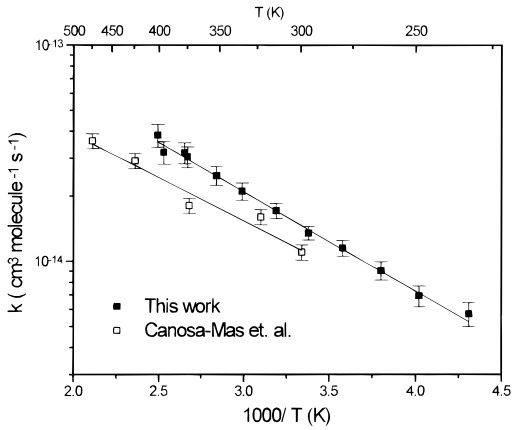

Figure 5. Arrhenius plots of k_2 (log scale) vs $1/T$ for 1-butene + NO_3 reaction: ■, our data; □, data from Canosa-Mas *et al.*[16] The lines represent weighted Arrhenius fits to the data. The error bars include precision and estimated systematic errors as mentioned in the text.

TABLE 2: Rate Coefficients (in Units of cm^3 molecule^{-1} s^{-1}) for Reaction of NO_3 with 1-Butene and Pertinent Experimental Conditions[a]

temp (K)	10^{14} × rate coefficient	pressure (Torr)	flow velocity (cm s^{-1})	[1-butene]/[NO_3]	wall coating
232	0.57 ± 0.06	2.4	480	34−850	wax[b]
249	0.69 ± 0.07	2.4	520	38−780	wax[b]
263	0.9 ± 0.09	2.4	550	65−680	wax[b]
279	1.15 ± 0.09	2.4	600	75−700	wax[b]
296	1.30 ± 0.10	2.4	825	80−581	wax[b]
296	1.38 ± 0.10	2.4	950	80−460	Teflon
296	1.35 ± 0.10	2.5	850	50−540	none
296	1.34 ± 0.10	8.4	900	85−450	none
296	1.34 ± 0.10	2.6	800	60−700	none
314	1.71 ± 0.14	2.5	1000	55−655	none
333	2.25 ± 0.19	2.4	1033	50−350	Teflon
334	1.88 ± 0.19	8.2	950	60−700	none
334	1.92 ± 0.19	2.5	920	65−530	none
352	2.48 ± 0.25	2.5	1100	50−600	none
374	3.03 ± 0.31	2.5	1200	50−510	none
377	3.16 ± 0.33	2.6	1100	53−590	Teflon
396	3.18 ± 0.35	2.5	1250	65−620	none
401	3.82 ± 0.42	2.4	1200	56−595	Teflon

[a] The error bars include precision and estimated systematic (2σ) errors. [b] Wax = halocarbon wax.

1-Butene + NO_3. The reaction of 1-butene with NO_3 was studied between 232 and 401 K, with either an uncoated wall, a Teflon sleeve (297−400 K) or a halocarbon wax coating (232−297 K). The results are shown in Figure 5 (solid squares) with the experimental uncertainty, which includes systematic and precision (2σ) errors. Table 2 lists the experimental conditions and results of these experiments. Also shown in the figure (open squares) are the data of Canosa-Mas *et al.*[16] The solid lines are, again, Arrhenius fits to the data. The Arrhenius parameters for reaction 2 in the range 232−401 K are $A = 5.2 \times 10^{-13}$ cm^3 molecule^{-1} s^{-1}, $E_a = -2120$ cal mol^{-1}, $\Delta E_a = 60$ cal mol^{-1} and $f(298) = 1.07$, with $k_2(298\text{ K}) = (1.4 \pm 0.10) \times 10^{-14}$ cm^3 molecule^{-1} s^{-1}. The quoted errors are at the 95% confidence level.

As in the case of reaction 1, high loss rate coefficients of NO_3 were observed when Teflon or bare walls were used at $T < 280$ K and caused deviation from the expected Arrhenius behavior. Such high loss rate coefficients were not observed when halocarbon wax was used. As a result, the low-temperature rate coefficients were obtained using halocarbon

TABLE 3: Rate Coefficients (in Units of cm^3 molecule^{-1} s^{-1}) at 298 K and Arrhenius Parameters for Reactions Studied in This Work and Those for Some Closely Related Reactions from Literature

compound	k(298 K)	A	E/R (K)	ref
2-methyl-3-butene-2-ol (MBO)	$(1.2 \pm 0.09) \times 10^{-14}$	4.6×10^{-14}	400	this work
1-butene	$(1.4 \pm 0.1) \times 10^{-14}$	5.2×10^{-13}	1070	this work
	$(1.4 \pm 0.3) \times 10^{-14}$ [a]			Japar and Niki[19]
	$(1.3 \pm 0.3) \times 10^{-14}$ [a]			Andersson and Ljunstrom[20]
	$(1.2 \pm 0.2) \times 10^{-14}$			Atkinson[17]
	$(1.3 \pm 0.2) \times 10^{-14}$			Barnes[18]
	$(1.1 \pm 0.2) \times 10^{-14}$	2.50×10^{-13}	940	Canosa-Mas *et al.*[16]
	1.2×10^{-14}	2.04×10^{-13}	843	Atkinson[2,3]
trans-2-butene	3.9×10^{-13}	1.1×10^{-12}	310	Atkinson[2,3]
methacrolein (MACR)	$<8 \times 10^{-15}$			this work
methyl vinyl ketone (MVK)	$<1.2 \times 10^{-16}$			this work
2-methyl-1,3-butadiene (isoprene)	6.78×10^{-13}	3.03×10^{-12}	446	Atkinson[2,3]
ethene	2.05×10^{-16}			Atkinson[2,3]
propene	9.49×10^{-15}	4.59×10^{-13}	1156	Atkinson[2,3]
2-methylpropene	3.32×10^{-13}			Atkinson[2,3]

[a] Calculated using the currently accepted value[14] for the equilibrium constant for $N_2O_5 \rightleftarrows NO_3 + NO_2$.

wax coating on the flow tube inner wall. For the high-temperature experiments, either Teflon or uncoated walls were used. We again attribute the high losses at low temperatures to enhanced reactions of NO_3 with 1-butene adsorbed on the wall of the flow tube.

Methyl Vinyl Ketone and Methacrolein + NO_3. In addition to reactions 1−3, we also measured rate coefficients for the reactions of NO_3 with methyl vinyl ketone (MVK) and methacrolein (MACR), two oxygenated hydrocarbons of natural origin. These studies were carried out at 298 K only, with a halocarbon-wax-coated flow tube. Only upper limits to the rate coefficients were obtained: $k_4(298\ \text{K}) \leq 1.2 \times 10^{-16}$ cm^3 molecule^{-1} s^{-1} and $k_5(298\ \text{K}) \leq 8.0 \times 10^{-15}$ cm^3 molecule^{-1} s^{-1}. Although we measured $k_4(298\ \text{K}) = (1.0 \pm 0.2) \times 10^{-16}$ cm^3 molecule^{-1} s^{-1}, we report an upper limit because our experiment is not suited to accurately measuring such low rate coefficients. We report only the upper limit for k_5, since the commercial MACR sample contained methylhydroquinone and acetic acid as inhibitors. We distilled the sample twice at a temperature of 250 K to collect pure MACR. Methylhydroquinone and acetic acid, which have low vapor pressures, are unlikely to be present in the purified sample. However, gas chromatographic analysis of the distilled samples revealed that some impurities that were in the original sample remained after distillation. Some of these impurities were identified to be cyclohexene, octene, methanol, propanol, and 2-methyl-2-butenal, all at less than 1 ppmv. The existence of these impurities at such low concentrations is not likely to increase the values of k_5. Since we were not able to obtain a much purer sample, we quote only an upper limit for k_5. The value of k_5 at 298 K using a doubly distilled sample was the same as that measured with the original sample.

Discussion

The most likely sources of errors in our measurements of k_1-k_5 are the occurrence of unrecognized secondary reactions, the determination of the concentrations of the excess reagent, impurities in the excess reagents, and the precision of the measurements.

Reactions other than (1)−(5), which either consume NO_3 or regenerate it, can introduce errors. The likely candidates that can consume NO_3 are the reactions of the NO_3 radicals with the products of the reactions. For example, if these reactions occur on every collision, because of the large initial concentrations of NO_3 employed here, the measured rate coefficient can be overestimated by a factor of 2 or more. The concentration of the NO_3 radical was $\sim 10^{12}$ cm^{-3}. Yet, the measured rate coefficients were not affected by any secondary reactions of NO_3. Experimentally, the insignificance of NO_3 side reactions was shown by the exponential nature of the $[NO_3]$ vs time (reaction distance) profiles and the invariance of the measured values of k_1-k_5 with the initial concentration of the NO_3 free radicals. Addition of O_2, which can scavenge the radicals formed in the reaction, did not alter the measured values of the rate coefficients as well. NO_3 does not undergo self reaction, and any reactions of NO_3 with the products of reactions 1−5 are unlikely to be fast enough to influence the measured rate constants.

The major problem associated with these measurements was the wall reactions at low temperatures. As discussed earlier, coating the walls with halocarbon wax minimized this effect. The linearity of the Arrhenius plots for reactions 1 and 2 bears this out. The identification that the enhanced rate coefficients at the lower temperatures were due to wall reactions was clearly shown by the departure from Arrhenius behavior occurring rather abruptly and the changes in the rate constants with the coating on the wall. Previous investigations have shown that halocarbon coating is a very good way to reduce the wall losses. Furthermore, one series of experiments carried out using pulsed photolytic production of NO_3 (by photolysis of N_2O_5 or $ClONO_2$) followed by its laser-induced fluorescence detection also yielded the same values for k_1 at 298 K. Because of the difficulties encountered due to dark side reactions between the NO_3 precursors and MBO, which were possibly heterogeneous in nature, we did not pursue this approach further.

Another source of possible error is the determination of the concentration of the excess reagent. The absorption cross sections of the reactants used in this study were too small to allow direct measurement of their concentrations in the gas mixture using absorption. Therefore, we used calibrated mass flow meters to determine their concentrations. As was discussed in the Results section, we estimate the uncertainty in this concentration to be 7%.

Table 3 lists our measured values of k_1-k_5 along with previous determinations of some of these rate coefficients. To our knowledge, k_1, k_4, and k_5 have not been measured before. Therefore, it is instructive to compare our results to the rate coefficients for NO_3 reactions with compounds containing similar functional groups.

The room temperature value of k_2 has been previously measured using many techniques[17−20] and, hence, provides a benchmark for comparison. Atkinson *et al.*[17] measured k_2 at 298 K to be $k_2(298\ \text{K}) = (1.23 \pm 0.2) \times 10^{-14}$ cm^3 molecule^{-1} s^{-1} by monitoring the loss of 1-butene relative to *trans*-2-butene

and assuming $k_3 = 3.89 \times 10^{-13}$ cm^3 molecule^{-1} s^{-1}. Barnes *at al.*[18] used propene ($k = 9.4 \times 10^{-15}$ cm^3 molecule^{-1} s^{-1}) as their standard and obtained $k_2(298\ \text{K}) = (1.3 \pm 0.2) \times 10^{-14}$ cm^3 molecule^{-1} s^{-1}. Japar and Niki[19] and Andersson and Ljungstrom[20] observed the rate of decay of N_2O_5, which was in equilibrium with NO_3, as a function of added 1-butene. By assuming that N_2O_5 does not react with 1-butene, they calculated $k_2(300\ \text{K}) = (7.8 \pm 0.8) \times 10^{-15}$ and $k_2(296\ \text{K}) = (6.4 \pm 0.3) \times 10^{-15}$ cm^3 molecule^{-1} s^{-1}. A reanalysis of their results using the currently recommended value[14] for the equilibrium constant for the process $N_2O_5 \rightleftarrows NO_3 + NO_2$, $k_{eq}(T) = 2.7 \times 10^{-27}e^{(11\,000/T)}$, yields $k_2 = (1.4 \pm 0.3) \times 10^{-14}$ and $k_2 = (1.3 \pm 0.3) \times 10^{-14}$ cm^3 molecule^{-1} s^{-1}, respectively. These rate coefficients are in excellent agreement with our 298 K value (Table 3). The rate coefficients measured by Canosa-Mas *et al.*[16] between 300 and 473 K are approximately 20% lower than our values as shown in Figure 5 (open triangles), even though they overlap with ours within the combined error limits. One possible reason for the higher values is the presence of impurities in our sample of 1-butene. We analyzed our sample using gas chromatography for possible impurities and found the level of impurities in our sample to be <0.5%. We did not observe any alkenes larger than butene. Therefore, we are confident that our values are not significantly affected by presence of impurities.

There is a lot of evidence that suggests that the reaction of NO_3 with alkenes proceeds by addition of NO_3 to the C=C double bond. Significant deuterium effect is not observed in the reaction of NO_3 with propene-d_6,[19] suggesting that abstraction of an H atom by NO_3, although exothermic, does not occur.[3,2] The products of NO_3 reactions with alkenes also suggest that the reaction involves addition of the NO_3 radical to the double bond with simultaneous π-bond rupture to form a nitrate radical adduct.[21−23] This reaction mechanism resembles the behavior of OH and O(^{3}P) reactions, which are known to be electrophilic additions. Since NO_3 has a higher electron affinity, EA, than those of both the OH radical and O(^{3}P) (EA(NO_3) ∼ 3.9 eV,[24,25] EA(OH) ∼ 1.83 eV,[26] and EA(O(^{3}P)) = 1.46 eV[27]), it is expected to react predominantly via electrophilic addition. Thus, the reactivity should be governed by the electron density distribution along the double bond and by steric factors.[2,3,16,19] NO_3 addition takes place on the least substituted carbon atom, and the rate coefficient at 298 K for the reaction increases with the amount of substitution with electron-donating groups, such as alkyl side chains, consistent with the inductive effect of the alkyl groups, which alters the electron distribution on the π-bond.[3,16] The presence of substituents also stabilize the radical formed following the NO_3 addition.

Atkinson has shown that there is a correlation between the rate coefficients of the reactions of NO_3 and OH with alkenes.[3] A similar comparison shows a correlation with the reactions of O(^{3}P).[28] It can be seen (Table 4) that less substituted hydrocarbons (such as ethene, propene, and 1-butene) react much more slowly than 2-alkenes and substituted alkenes. Alkyl substitution on the double bond enhances the reactivity (*cis*- and *trans*-butene), but steric hindrance slows it down. Furthermore, substitution by another alkyl group enhances the reactivity even more (2-methyl-2-butene). Also, for less substituted alkenes, the OH reactions are much faster than the corresponding NO_3 reactions. However, in branched alkenes the NO_3 reaction becomes comparable to the OH reaction. To our knowledge, the effect of an electron-withdrawing group such as alcohol or aldehyde has not been previously compared. Yet, the overall reactivity of reaction 1 is consistent with NO_3 addition to the double bond in MBO.

TABLE 4: Rate Coefficients (in Units of cm^3 molecule^{-1} s^{-1}) at 298 K for Reactions of NO_3, OH, and O(^{3}P) with Some Simple Alkenes

compound	k(298 K) for NO_3[a] × 10^{14}	k(298 K) for OH[b] × 10^{12}	k(298 K) for O(^{3}P)[c] × 10^{12}
ethene	0.02	8.52	0.44
propene	0.95	26.3	3.98
2-methylpropene	33.2	51.4	16.9
methacrolein (MACR)	≤0.01	20.0	
1-butene	1.4[d]	31.4	4.15
2-methyl-3-butene-2-ol (MBO)	1.2[d]	64.0[e]	
cis-2-butene	33.2	56.4	17.6
trans-2-butene	39.0	64.0	21.7
2-methyl-2-butene	937	86.9	56.5

[a] Reference 2. [b] Reference 2. [c] Reference 28. [d] This work. [e] Reference 8.

Both steric and inductive effects may play a role in determining the reactivity of NO_3 with MBO. The alcohol group, which is an electron-withdrawing group, can reduce the electron density across the double bond and, hence, slow the reaction. In addition, the methyl and alcohol groups on the β-carbon atom to the double bond may pose a steric hindrance to the double bond site. These factors probably determine the rate by which reaction 1 can proceed. In 1-butene, on the other hand, steric hindrance should not be significant. This might be the reason that 1-butene reacts slightly faster than MBO. Since the OH group in MBO is not directly bonded to the carbon−carbon double bond, its effect on the reactivity is not very large but still noticeable. We speculate that the difference in reactivity arises mainly because of the steric hindrance, which is also reflected in a smaller Arrhenius pre-exponential factor (∼5×10^{-14} as opposed to ∼5×10^{-13} cm^3 molecule^{-1} s^{-1} for 1-butene). The inductive effect due to the highly substituted β-carbon may be the reason that the activation energy observed for MBO is lower than that of 1-butene.

The effect of the oxygenated substituents can be best seen by comparing a list of compounds of similar structure. By looking at Table 4, one can observe that the reactivity decreases in the following order: 2-methylpropene ≫ propene > MACR for substituted propenes. In 2-methylpropene, the methyl group, which is an electron-donating group, enhances the reactivity compared to propene. When a propene is substituted with an aldehyde group in MACR, the reactivity is decreased. For butenes, a similar trend is observed: 2-methyl-2-butene ≫ *trans*-2-butene > 1-butene > MBO. 2-Methyl-2-butene has three alkyl substituents on the double bond, and hence, it reacts very fast. *trans*-2-Butene has one methyl group on each double bonded carbon, and it reacts a little more slowly. 1-Butene and MBO have only one alkyl substitution on the double bonded carbon, and they react even more slowly. In MBO, the OH group is probably decreasing the reactivity; however, since it is not directly attached to the double bond, the effect is not very large. MVK can be considered to be an ethene substituted with a carbonyl group (an electron withdrawing functional group) to the double bond which makes its reaction slower than that of ethene.

Rate coefficients k_1 and k_2 do not increase with pressure in the small pressure range over which they were studied (1−15 Torr (133 - 200 Pa)). The lack of pressure dependence is consistent with other NO_3 reactions of this type, whose rate coefficients do not change with pressure.[3,1]

TABLE 5: Comparison of the Atmospheric Lifetimes of Compounds Investigated Here[f]

	rate coefficient (cm^3 $molecule^{-1}$ s^{-1})			atmosphere lifetime (hours)		
	k_{OH}	k_{O_3}	k_{NO_3}	τ_{OH}	τ_{O_3}	τ_{NO_3}
2-methyl-1,3-butadiene (isoprene)	1.01×10^{-10} [a]	1.15×10^{-17} [a]	6.78×10^{-13} [a]	2.9	24	0.8
methyl vinyl ketone (MVK)	1.88×10^{-11} [b]	4.56×10^{-18} [a]	$\leq 1.2 \times 10^{-16}$ [c]	14	60.6	>4610
methacrolein (MACR)	2.01×10^{-11} [b]	1.14×10^{-18} [a]	$\leq 8.0 \times 10^{-15}$ [c]	14	245	>72
2-methyl-3-butene-2-ol (MBO)	6.40×10^{-11} [d]	1.00×10^{-17} [e]	1.20×10^{-14} [c]	4.3	27	46

[a] References 2 and 3. [b] Reference 32. [c] This work. [d] Reference 8. [e] Reference 9. [f] Reactions with OH, ozone, and the nitrate radical are considered. Rate coefficients units are cm^3 $molecule^{-1}$ s^{-1} and lifetimes are in hours. Assumptions: $[OH] = 1.0 \times 10^6$, $[O_3] = 1.0 \times 10^{12}$, $[NO_3] = 5 \times 10^8$ cm^{-3}.

Atmospheric Implications. Table 5 lists the tropospheric lifetimes of several compounds of natural origin due to reaction with the OH radical, ozone, and the nitrate radical.

MBO was recently discovered to be present in the atmosphere in high concentrations, up to 8 ppbv.[4] Although its exact origin has not been fully identified, the similarity in its diurnal behavior and the correlation of its concentration with that of isoprene suggest that it is emitted by a vegetative source. In a previous study,[8] we have found that the reaction of MBO with OH is fast, with a rate constant of 6.4×10^{-11} cm^3 $molecule^{-1}$ s^{-1} at 298 K. Grosjean and Grosjean[9] reported the rate coefficient for the ozone + MBO reaction at 291 K to be 1.0×10^{-17} cm^3 $molecule^{-1}$ s^{-1}. With the 298 K rate coefficient of 1.2×10^{-14} cm^3 $molecule^{-1}$ s^{-1} for the NO_3 + MBO reaction we conclude that the atmospheric lifetime of MBO will be dominated by the reaction with OH. At night, reaction of MBO with ozone is comparable to the loss due to reaction with NO_3 in clean areas, where NO_3 concentrations are low. For example, assuming $[NO_3] = 5 \times 10^8$ cm^{-3} and $[O_3] = 1 \times 10^{12}$ cm^{-3} (40 ppbv at atmospheric pressure), reaction 1 is responsible for about 40% of the MBO loss during the night. However, since the emission of MBO is light-mediated,[4] and since the reaction with OH is fast, the concentrations of MBO during the night are expected to be low and the main loss of MBO would be during the day by the reaction with OH.

Isoprene is the most abundant emission from vegetation, while MVK and MACR are two of the main photochemical degradation products of isoprene.[29] Removal of MVK by the NO_3 reaction is not significant, and the reaction with ozone will dominate its nighttime loss (see Table 5). For MACR, however, the nighttime removal may be via the NO_3 reaction. In a few field campaigns,[29,30] nighttime MACR concentrations were reported to be slightly higher than that of MVK, in contrast to the daytime behavior where [MVK] > [MACR]. This behavior can be rationalized by different nighttime removal rates. MVK is removed by ozone alone faster than the removal of MACR by ozone and NO_3 reactions together. This will result in a faster removal of MVK than of MACR during the night and might lead to its lower nighttime concentrations, consistent with the observations.[29,30]

1-Butene is produced mainly by anthropogenic activities, and its concentration in the atmosphere can be as high as 350 ppbv in polluted atmospheres[16] and as low as a few ppbv in remote places.[31] The lifetime of 1-butene due to reaction with NO_3 is about 30 h (assuming $[NO_3] = 5 \times 10^8$ cm^{-3}). The tropospheric lifetime of 1-butene due to the reaction with OH is about 10 h (assuming $[OH] = 10^6$ cm^{-3}, $k(298\ K) = 3.14 \times 10^{-11}$ cm^3 $molecule^{-1}$ s^{-1}) and that with ozone is about 30 h (assuming $[O_3] = 1 \times 10^{12}$ cm^{-3}, $k(298\ K) = 9.64 \times 10^{-18}$). During the day, 1-butene will be lost by reaction with the OH radical (~75%) and by reaction with ozone (~25%). At night, NO_3 may be responsible for ~40% of the 1-butene nighttime loss. All of these numbers should be treated with caution because the NO_3 and OH concentrations vary substantially, depending on the environment, location, and season.

Acknowledgment. We thank Steve Montzka of NOAA/CMDL in Boulder for performing the GC−MS analysis of the MBO, MACR, and MVK samples and Stephen Barone for performing the PP−LIF experiment of NO_3 with MBO. This work was performed while Yinon Rudich held a National Research Council−NOAA Research Associateship. This research was funded in part by NOAA's Climate and Global Change research program.

References and Notes

(1) Wayne, R. P.; Barnes, I.; Biggs, P.; Burrows, J. P.; Canosa-Mas, C. E.; Hjorth, J.; Le Bras, G.; Moortgat, G. K.; Perner, D.; Poulet, G.; Restelli, G.; Sidebottom, H. *Atmos. Environ.* **1991**, *25A*, 1.

(2) Atkinson, R. *J. Phys. Chem. Ref. Data Monogr. 2*, **1994**.

(3) Atkinson, R. *J. Phys. Chem. Ref. Data* **1991**, *20*, 459.

(4) Goldan, P. D.; Kuster, W. C.; Fehsenfeld, F. C.; Montzka, S. A. *Geophys. Res. Lett.* **1993**, *20*, 1039.

(5) Cardelino, C. A.; Chameides, W. L. *J. Geophys. Res.* **1990**, *95*, 13971.

(6) Chameides, W. L.; Lindsay, R. W.; Richardson, J.; Kiang, C. S. *Science* **1988**, *241*, 1473.

(7) Fehsenfeld, F.; Calvert, J.; Fall, R.; Goldan, P.; Guenther, A. B.; Hewitt, N.; Lamb, B.; Liu, S.; Trainer, M.; Westberg, H.; Zimmerman, P. *Global Biogeochem. Cycles* **1992**, *6*, 389.

(8) Rudich, Y.; Talukdar, R. K.; Burkholder, J. B.; Ravishankara, A. R. *J. Phys. Chem.* **1995**, *99*, 12188.

(9) Grosjean, E.; Grosjean, D. *Int. J. Chem. Kinet.* **1994**, *26*, 1185.

(10) White, J. U. *J. Opt. Soc. Am.* **1942**, *32*, 285.

(11) White, J. U. *J. Opt. Soc. Am.* **1976**, *66*, 411.

(12) Howard, C. J. *J. Phys. Chem.* **1979**, *83*, 3.

(13) Tyndall, G. S.; Orlando, J. J.; Cantrell, C. A.; Shetter, R. E.; Calvert, J. G. *J. Phys. Chem.* **1991**, *95*, 4381.

(14) DeMore, W. B.; Sander, S. P.; Golden, D. M.; Hampson, R. F.; Kurylo, M. J.; Howard, C. J.; Ravishankara, A. R.; Kolb, C. E.; Molina, M. J. Chemical Kinetics and Photochemical Data for use in Stratospheric Modeling, Evaluation No. 11. JPL Publication 94-26; Jet Propulsion Laboratory: Pasadena, CA, 1994.

(15) Dlugokencky, E. J.; Howard, C. J. *J. Phys. Chem.* **1989**, *93*, 1091.

(16) Canosa-Mas, C. E.; Monks, P. S.; Wayne, R. P. *J. Chem. Soc., Faraday Trans.* **1992**, *88*, 11.

(17) Atkinson, R.; Aschmann, S. M.; Pitts, J. N., Jr. *J. Phys. Chem.* **1988**, *92*, 3454.

(18) Barnes, I.; Bastian, V.; Becker, K. H.; Tong, Z. *J. Phys. Chem.* **1990**, *94*, 2413.

(19) Japar, S. M.; Niki, H. *J. Phys. Chem.* **1975**, *79*, 1629.

(20) Andersson, Y.; Ljungstrom, E. *Atmos. Environ.* **1989**, *23*, 1153.

(21) Benter, T.; Liesner, M.; Schindler, R. N.; Skov, H.; Hjorth, J.; Restelli, G. *J. Phys. Chem.* **1994**, *98*, 10492.

(22) Skov, H.; Betner, T.; Schindler, R. N.; Hjorth, J.; Restelli, G. *Atmos. Environ.* **1994**, *28*, 1583.

(23) Olzmann, M.; Betner, T.; Liesner, M.; Schindler, R. N. *Atmos. Environ.* **1994**, *128*, 2677.

(24) Davidson, J. A.; Fehsenfeld, F. C.; Howard, C. J. *Int. J. Chem. Kinet.* **1977**, *9*, 17.
(25) Weaver, A.; Arnold, D. W.; Bradforth, S. E.; Neumark, D. M. *J. Chem. Phys.* **1991**, *94*, 1740.
(26) Schulz, P. A.; Mead, R. D.; Jones, P. L.; Lineberger, W. C. *J. Chem. Phys.* **1982**, *77*, 1153.
(27) Neumark, D. M.; Lyke, K. R.; Andersen, T.; Lineberger, W. C. *Phys. Rev. A.* **1985**, *32*, 1890.
(28) Cvetanovic, R. J. *J. Phys. Chem. Ref. Data* **1987**, *16*, 261.
(29) Montzka, S. A.; Trainer, M.; Goldan, P. D.; Kuster, W. C.; Fehsenfeld, F. C. *J. Geophys. Res.* **1993**, *98*, 1101.
(30) Montzka, S. A.; Trainer, M.; Angevine, W. A.; Fehsenfeld, F. C. *J. Geophys. Res.* **1995**, *100*, 11393.
(31) Penkett, S. A.; Blake, N. J.; Lightman, P.; Marsh, A. R. W.; Anwyl, P.; Butcher, G. *J. Geophys. Res.* **1993**, *98*, 2865.
(32) Talukdar, R. K.; Burkholder, J. B.; Gierczak, T.; Mellouki, A.; Barone, S.; Ravishankara, A. R. In preperation.

JP953079G